Crack-Resistant Zirconia-Based Composite Ceramics with Increased Hardness of the Near-Surface Layer

A. A. Dmitrievskiy[a], *, D. G. Zhigacheva[a], N. Yu. Efremova[a], V. M. Vasyukov[a], and G. V. Grigoriev[a]

[a] Derzhavin Tambov State University, Tambov, 392000 Russia
*e-mail: aadmitr@yandex.ru

Abstract—Using a relatively economical method of powder metallurgy, a two-layer composite ceramic based on zirconia stabilized with calcium oxide and alumina toughened (Ca-ATZ) is fabricated. One of the layers contains an additive of silicon dioxide (Ca-ATZ + SiO_2). The structure and elemental and phase composition, as well as the set of mechanical properties of the samples in the vicinity of the Ca-ATZ/Ca-ATZ + SiO_2 layer interface are studied. It is shown that the presence of a sharp interface between layers with different elemental compositions does not cause structural damage (appearance of pores, cracks, and other macroscopic defects that contribute to deterioration of the strength properties) or changes in the phase composition (more than 90% of zirconia in both layers is in the tetragonal phase, which ensures a high role of the transformation toughening mechanism). The demonstrated preservation of the structural integrity and the ratio of the monoclinic, tetragonal, and cubic phases of zirconia during the formation of a sharp interface between these layers makes it possible to fabricate ceramic based on zirconium dioxide with a thin (100−200 μm) modified layer. Taking into account the difference in the mechanical properties of Ca-ATZ and Ca-ATZ + SiO_2 ceramic, this provides a base material (containing SiO_2) with increased fracture toughness (not less than 12 MPa m$^{1/2}$) and a surface layer (containing no SiO_2) with nanohardness (no lower than 14 GPa).

Keywords: two-layer composite ceramic, microstructure, phase composition, surface modification, hardness, fracture toughness, interface compositions

DOI: 10.1134/S1027451023040250

INTRODUCTION

Controlling the composition (elemental and/or phase) and structure of structural materials makes it possible to vary their properties in a wide range, including mechanical properties. As a rule, the improvement of some characteristics (for example, hardness) is accompanied by the deterioration of others (for example, fracture toughness) and vice versa. Therefore, researchers often resort to modification (of the composition or structure) not of the entire bulk of the material, but of its surface layers [1]. This provides improvement in the properties important for the surface layers (hardness, friction coefficient, etc.) while maintaining properties important for the bulk of the material (Young's modulus, fracture toughness, etc.).

There are various methods for modifying the structure of the surface layers of materials. Methods of mechanical [2], radiation [3, 4], laser [5], and chemical [6] processing, and some other types of influences [7, 8] have become widespread. The introduction of additives into the composition of the surface layer, i.e., changing its elemental composition, is also an effective method for modifying properties. Materials, in which the composition (and, as a result, properties) change smoothly or step by step from the surface to the volume, represent a special class of composite materials. They are called functionally graded materials [9–12].

From the point of view of the design and production of functionally graded materials, powder technologies are the most technologically simple and reliable [10, 13]. This approach is widely used in the manufacture of functionally graded ceramic. Taking into account the unique set of mechanical properties, chemical, thermal, and radiation resistance, as well as bioinertness, alumina toughened zirconia functionally graded ceramic (ATZ ceramic) [14, 15] is of great interest. In [16−18], we showed that the introduction of silicon dioxide (~4.5−5 mol %) into ATZ ceramic results in an increase in fracture toughness (by 75%), compressive strength (by 14%), and also the appearance of signs of plasticity (stage of fluidity in the process of uniaxial compression at room temperature). However, unfortunately, such an additive leads to a decrease in hardness by 14%. The combination of two materials (ATZ ceramic containing and lacking SiO_2) can provide one layer (for example, the main bulk of the material) with increased values of fracture toughness and compressive strength, as well as a margin of plasticity at room temperature, and the other (surface layer) with high hardness.

In this regard, the aim of the study is to manufacture a monolithic two-layer (containing and lacking silicon dioxide) alumina toughened zirconia ceramic and to study its structure and the set of mechanical properties.

EXPERIMENTAL

Monolithic two-layer samples of Ca-ATZ/Ca-ATZ + SiO_2 ceramic were made from two preliminarily prepared powder mixtures. The first mixture contained ZrO_2 (Sigma-Aldrich), Al_2O_3 (Hongwu), and CaO (Reachem) powders. The second mixture contained additionally 5 mol % of SiO_2 powder (Sigma-Aldrich).

The ratio of the molar concentrations of the components of the initial mixtures was kept close to those described in [16]. The powder mixtures were alternately poured into the mold so that the surface of each of them was even. Molding and sintering of the samples was carried out by analogy with [16].

The surface of the samples was visualized using an Axio Observer A1m (Carl Zeiss) inverted optical microscope and a Merlin (Carl Zeiss) high-resolution scanning electron microscope. Elemental mapping was carried out using a JCM-7000 (JEOL) scanning electron microscope. The phase composition of the end surfaces of the cylindrical samples was studied using a D2 Phaser X-ray diffractometer (Bruker AXS). The average crystallite size (or coherent-scattering region) d was calculated from the broadening of the diffraction peaks using the Scherrer equation.

To reveal changes in the mechanical properties from the surface to the bulk, the samples were cut perpendicular to the surface. The structure and mechanical properties were studied on the formed surface (Fig. 1a). The nhardness H was determined by nanoindentation (Berkovich pyramid) using a NanoIndenter G200 nanoindenter (MTS NanoInstruments).

To determine the fracture toughness of K_{1C} by indentation (Vickers pyramid, load was 50 N), an automated Duramin-A300 microhardness tester (EmcoTest) was used. The K_{1C} value was determined according to [19] from the expression:

$$K_{1C} = 0.016(E/H_v)^{0.5}/(P_v/l^{1.5}),\qquad(1)$$

where E is Young's modulus, H_v is the microhardness measured using the Vickers pyramid, P_v is the maximum load on the indenter during the formation of the Vickers indent, and l is the average length of radial cracks.

RESULTS AND DISCUSSION

Figure 1b shows an image obtained by scanning electron microscopy (SEM) of a section of the ceramic cleavage surface in the Ca-ATZ + SiO_2 layer.

It can be seen that the sizes of the aluminum oxide Al_2O_3 crystallites (darker in color) exceed the sizes of the ZrO_2 crystallites. This ensures the manifestation of the dispersion toughening mechanism, which amounts to dissipation of the energy of a propagating crack when rounding a harder obstacle [20]. In addition, traces of the transgranular destruction of ZrO_2 crystallites are visible indicating a high degree of intergranular interaction. The above allows one to expect an increased (relative to zirconia ceramic without additives) fracture toughness.

Comparative analysis of the distribution maps of Zr, Al, O, and Si along a section of the cross section of the Ca-ATZ/Ca-ATZ + SiO_2 ceramic (Figs. 1c−1f) clearly demonstrates the presence of a sharp boundary in the distribution of silicon dioxide over the sample volume. The presence of a signal from Si on the left part of the distribution map (Fig. 1f) is apparently due to the mechanical transfer of material from one part of the sample to another during grinding and polishing of the surface. Thus, it can be considered that the fabricated samples of Ca-ATZ/Ca-ATZ + SiO_2 ceramic have a sharp boundary in the distribution of silicon dioxide or silicon-containing compounds.

Figures 2a and 2b show diffraction patterns recorded at opposite end sides of a two-layer Ca-ATZ/Ca-ATZ + SiO_2 ceramic. It can be seen that the main reflections of both diffraction patterns belong to the tetragonal phase t-ZrO_2. Quantitative analysis of the obtained spectra made it possible to conclude that the relative proportions of the tetragonal phase t-ZrO_2 in both layers are the same and exceed 90% (Table 1). A high proportion of the tetragonal phase t-ZrO_2 in both layers ensures manifestation of the transformational toughening mechanism inherent in zirconia ceramic [21, 22]. The average sizes of t-ZrO_2 and Al_2O_3 crystallites also barely depend on the introduced SiO_2 additive (Table 1).

Despite the similarity of the structure and phase composition of the layers containing and lacking silicon dioxide, the presence of a sharp boundary between them ensures equally sharp changes in the micromechanical properties. As an example, Fig. 2c shows an image of an indenter imprint (Vickers pyramid) obtained using an Axio Observer A1m optical microscope. One half of the indenter (left) is in the layer of Ca-ATZ ceramic, the other (right) is in the layer of Ca-ATZ + SiO_2 ceramic.

It can be seen that the lengths of radial cracks in the right corners of the imprint are much smaller than those in the left corners. The calculation performed using expression (1) shows that the introduction of SiO_2 into ATZ ceramic provides an increase in fracture toughness K_{1C} by 30% (Table 1), which is due to an increase in the transformability (ability to phase transformation) of the t-ZrO_2 tetragonal phase and, as a
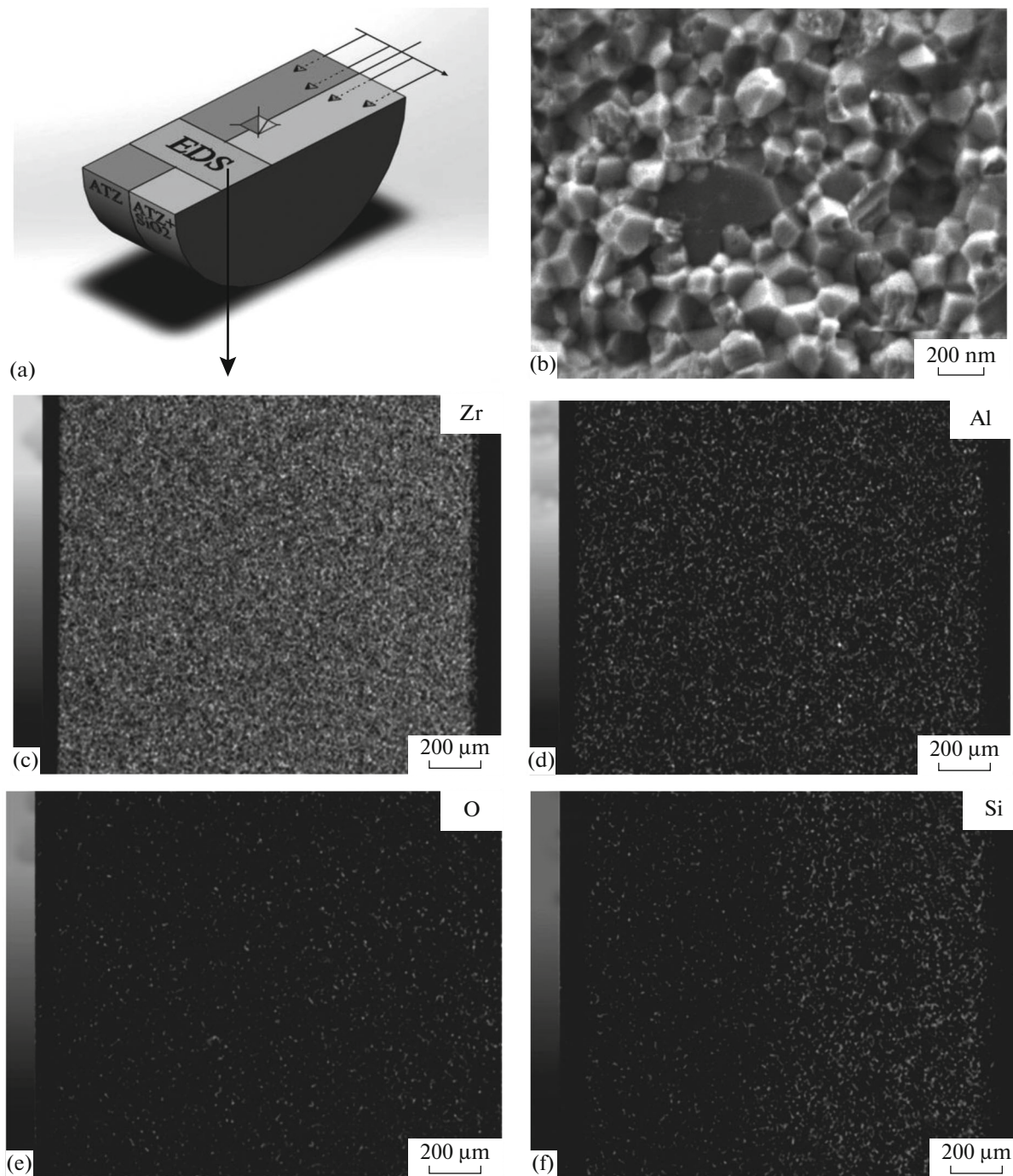
Fig. 1. (a) Schematic representation of the sample with the regions under study, (b) SEM image of the cleavage surface, (c)−(f) distribution maps of Zr, Al, O, and Si along the cross section of the sample, respectively.

consequence, an increase in the role of transformation toughening upon the addition of SiO_2 [16, 17].

Unfortunately, when silicon dioxide (5 mol %) is added to Ca-ATZ ceramic, an abrupt decrease in the nanohardness H is observed (Fig. 2d), which may have negative consequences for its practical applications as an engineering ceramic. This agrees with the earlier obtained data on a decrease in hardness upon the introduction of silicon dioxide into Ca-ATZ ceramic [16]. We note that the width of the transition layer (the range of Δr values, in which the abrupt change in H occurs), does not exceed 20 μm (Fig. 2e). Similar (jump-like) changes in the microhardness were observed by us earlier upon passing from zirconia ceramic (stabilized in the tetragonal phase with cal-
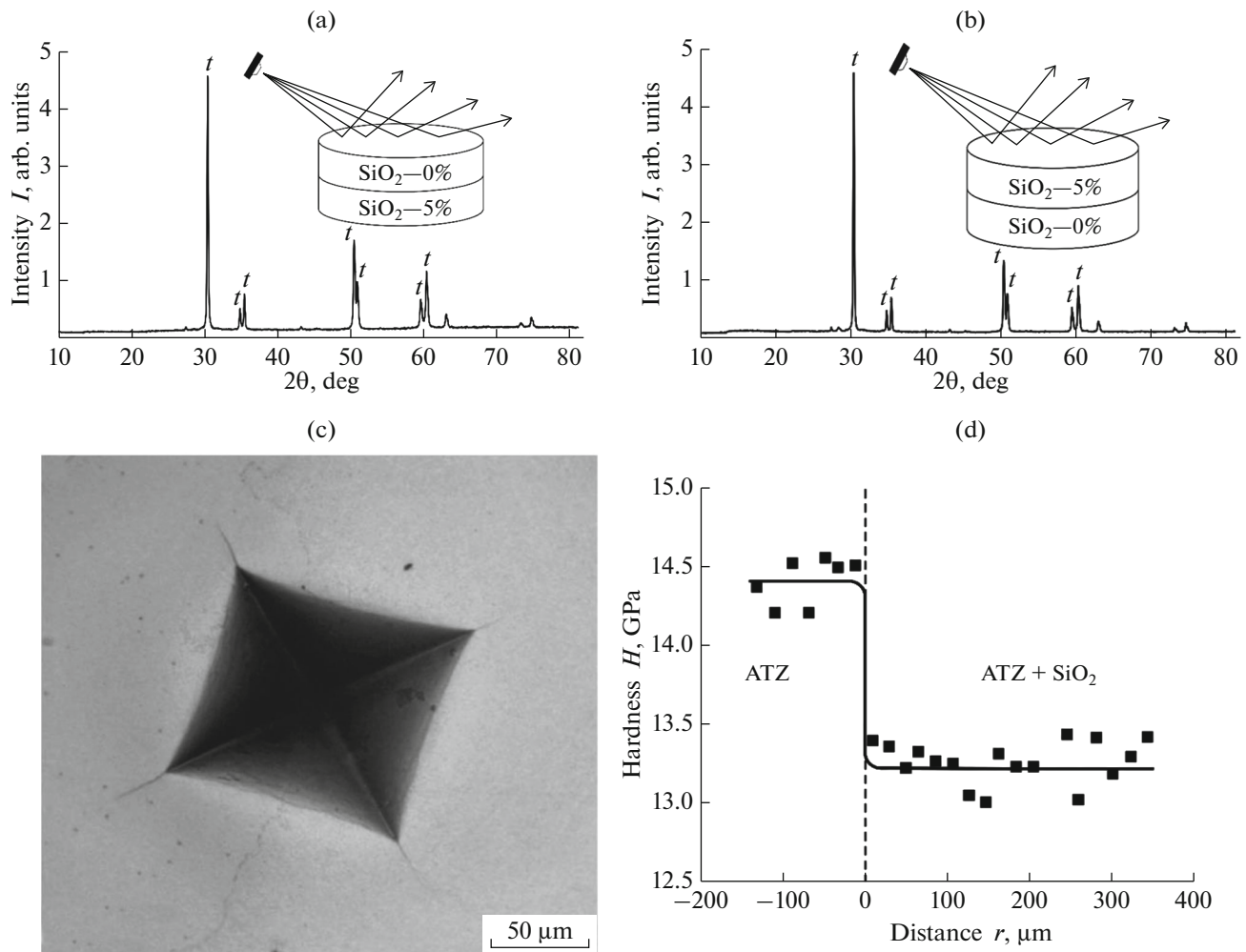
Fig. 2. X-ray diffraction patterns recorded in a layer (a) with zero and (b) five percent content of SiO_2, (c) image of a cross section with an indent of the Vickers pyramid formed at a load of $P_V = 50$ N, and (d) the dependence of the nanohardness H on the distance r to the interface between the Ca-ATZ and Ca-ATZ + SiO_2 layers.

cium oxide) to Ca-ATZ ceramic [18]. This shows the possibility of creating thin surface layers of Ca-ATZ ceramic with high hardness on Ca-ATZ + SiO_2 ceramic with increased fracture toughness. It should be noted that the achieved ratio of the nanohardness (in a thin surface layer that lacks SiO_2) and fracture toughness (bulk of the material containing SiO_2) exceeds similar ratios recorded on a zirconia-based composite ceramics without the addition of silicon dioxide, which are described in detail in [16].

CONCLUSIONS

The two-layer composite ceramic Ca-ATZ/CaATZ + SiO_2 with a sharp compositional interface ($\Delta r \leq 20$ μm) was fabricated. It was shown that the introduction of the SiO_2 additive into Ca-ATZ ceramic has almost no effect on the structure and phase composition. However, it causes an increase in fracture toughness by 30% with a decrease in nanohardness by 10%. Thus, the possibility of manufacturing Ca-ATZ + SiO_2 ceramic with increased crack resistance with a thin surface

Table 1. Relative fractions of monoclinic (m-), tetragonal (t-), and cubic (c-) phases of ZrO_2; sizes of ZrO_2 and Al_2O_3 crystallites d; Young's modulus E; nanohardness H, and fracture toughness K_{1C} of Ca-ATZ and Ca-ATZ + SiO_2 layers, as well as the relative density of the two-layer ceramic ρ

	m-ZrO_2%	t-ZrO_2%	c-ZrO_2%	d_{Zr}, nm	d_{Al}, nm	E, GPa	H, GPa	K_1c, MPa m$^{1/2}$	ρ, %
Ca-ATZ	3	92	5	85	190	235.7	14.4	9.1	99
Ca-ATZ + SiO_2	5	92	3	90	200	220.2	13.3	12.1	

layer containing no silicon dioxide (Ca-ATZ) and characterized by high hardness was shown.

CONFLICT OF INTEREST

The authors declare that they have no conflicts of interest.

REFERENCES

1. *Surface Modification of Biomaterials. Methods Analysis and Applications*, Ed. by R. Williams (Woodhead, New York, 2011).

2. *Surface Modification by Solid State Processing*, Ed. by R. Miranda (Woodhead, New York, 2014).

3. I. P. Jain and G. Agarwal, Surf. Sci. Rep. **66**, 77 (2011). https://doi.org/10.1016/j.surfrep.2010.11.001

4. R. F. Egerton, Micron **119**, 72 (2019). https://doi.org/10.1016/j.micron.2019.01.005

5. I. V. Ushakov, Proc. SPIE **6597**, 659714 (2007). https://doi.org/10.1117/12.726773

6. I. V. Ushakov, V. A. Feodorov, and I. J. Permyakova, Proc. SPIE **5400**, 265 (2004). https://doi.org/10.1117/12.555529

7. F. Tao, Y. Liu, X. Ren, J. Wang, Y. Zhou, Y. Miao, F. Ren, Sh. Wei, and J. Ma, J. Energy Chem. **66**, 397 (2022). https://doi.org/10.1016/j.jechem.2021.08.022

8. A. Alagatu, D. Dhapade, M. Gajbhiye, R. Panjrekar, and A. Raut, Mater. Today: Proc. **60**, 2245 (2022). https://doi.org/10.1016/j.matpr.2022.03.338

9. M. Koizumi, Ceram. Eng. Sci. Proc. **13**, 333 (1992). https://doi.org/10.1002/9780470313954.ch33

10. Y. Miyamoto, W. Kaisser, B. H. Rabin, A. Kawasaki, and R. G. Ford, *Functionally Graded Materials: Design, Processing, and Applications* (Springer, New York, 1999).

11. A. Pasha and B. M. Rajaprakash, Mater. Today: Proc. **52**, 379 (2022). https://doi.org/10.1016/j.matpr.2021.09.066

12. J. Sun, D. Ye, J. Zou, X. Chen, Y. Wang, J. Yuan, H. Liang, H. Qu, J. Binner, and J. Bai, J. Mater. Sci. Technol. **138**, 1 (2023). https://doi.org/10.1016/j.jmst.2022.06.039

13. M. Sam, R. Jojith, and N. Radhika, J. Manuf. Process. **68**, 1339 (2021). https://doi.org/10.1016/j.jmapro.2021.06.062

14. D. H. A. Besisa and E. M. M. Ewais, Mater. Res. Express **6**, 075516 (2019). https://doi.org/10.1088/2053-1591/ab177e

15. E. M. M. Ewais, D. H. A. Besisa, Z. I. Zaki, and A. E. H. T. Kandil, J. Eur. Ceram. Soc. **32**, 1561 (2012). https://doi.org/10.1016/j.jeurceramsoc.2012.01.016

16. A. A. Dmitrievskii, A. O. Zhigachev, D. G. Zhigacheva, and V. V. Rodaev, Tech. Phys. **65**, 2016 (2020). https://doi.org/10.1134/S1063784220120075

17. A. A. Dmitrievskiy, D. G. Zhigacheva, V. M. Vasyukov, and P. N. Ovchinnikov, J. Phys.: Conf. Ser. **2103**, 012075 (2021). https://doi.org/10.1088/1742-6596/2103/1/012075

18. A. A. Dmitrievskiy, D. G. Zhigacheva, G. V. Grigoriev, and P. N. Ovchinnikov, J. Surf. Invest.: X-ray, Synchrotron Neutron Tech. **15**, 137 (2021). https://doi.org/10.1134/S1027451022020264

19. G. R. Anstis, P. Chantikul, B. R. Lawn, and D. B. Marshall, J. Am. Ceram. Soc. **64**, 533 (1981). https://doi.org/10.1111/j.1151-2916.1981.tb10320.x

20. F. Zhang, L. F. Lin, and E. Z. Wang, Ceram. Int. **41**, 2417 (2015). https://doi.org/10.1016/j.ceramint.2015.06.081

21. R. C. Garvie, R. H. J. Hannink, and R. T. Pascoe, Nature **258**, 703 (1975). https://doi.org/10.1038/258703a0

22. R. H. J. Hannink, P. M. Kelly, and B. C. Muddle, J. Am. Ceram. Soc. **83**, 461 (2000). https://doi.org/10.1111/j.1151-2916.2000.tb01221.x

Translated by S. Rostovtseva